A study on the dynamic response of a semi-submersible floating offshore wind turbine system Part 2: numerical simulation

Pham Van Phuc[1)], Takeshi Ishihara[2)]

[1)]*Dept. of Civil Eng., The Univ. of Tokyo, 7-3-1 Hongo, Bunkyo, Tokyo, Japan*
[2)]*Institute of Eng., Innovation School of Eng., The Univ. of Tokyo, Tokyo, Japan*

ABSTRACT: A FEM code was developed to predict the dynamic behaviors of elastic floating offshore wind turbine systems in the time domain, employing the Morison's equation to calculate the hydrodynamic drag forces and inertia forces in the perpendicular to the columns of floater, and quasi-steady theory to calculate the aerodynamic forces on wind turbines. Since the relative velocities of the moving element were used to predict the drag forces, the hydrodynamic and aerodynamic damping were automatically taken into account during the simulation. The responses predicted by the proposed numerical model showed a good agreement with experiments, and those by the conventional numerical models were overestimated due to the lack of considering the interaction between wind turbines and floater. The elastic responses of the floater were investigated, and the peak responses were observed at resonant points around the natural periods of the deformation of the elastic model.

KEYWORDS: Floating offshore wind turbine system, Morison's equation, hydrodynamic damping, aerodynamic damping, drag force, elastic deformation.

1 INTRODUCTION

Evaluation of dynamic behaviors considering the interaction between floater and wind turbines is one of the important factors in the process of optimization and design of the floating offshore wind turbine systems. In order to investigate the dynamic behaviors of the floaters, there are two different approaches. One is the application of the so-called Morison's equation [1], and another is the linear potential theory [2], which were commonly used in civil engineering and oil & gas industry, respectively. Although, the linear potential theory is raised from the assumptions of zero viscosity of the fluid, the Morison's equation considers the effect of viscosity represented by the non-linear hydrodynamic drag force. Hederson et al. [1] used the Morison's equation for the floating structure with large diameter sub-structures, in which the hydrodynamic drag force would be small compared with the inertia force. They ignored the hydrodynamic drag force and solve the linearized equation of motion in the frequency domain. This simplification might lead some error to predict the dynamic behaviors of the light floaters with small diameter sub-structures, such as the floater proposed by Ishihara et al.[3]. The nonlinear hydrodynamic drag force can be linearized and solved the equation of motion with some iteration and incorporated into the linear potential theory in the frequency domain. However, the linearization might also lead to overestimate or underestimate the dynamic responses of the floaters.

In the present study, a FEM code based on the Morison's equation has been developed and solved in the time domain to consider the nonlinear terms such as nonlinear hydrodynamic and aerodynamic forces, nonlinear mooring, etc… and the interaction between wind turbines and floater. The performance of the code was verified in comparison with the experimental results obtained in the part 1 of this study. In order to investigate the effect of elastic deformations, the dynamic responses of elastic model were simulated and the results were compared with those of rigid model.

2 NUMERICAL METHOD OF FULL DYNAMIC SIMULATION

2.1 *Governing equation*

The general formulation of the differential equation of motion for a floating offshore wind turbine system can be written as

$$[M]\{\ddot{X}\}+[C]\{\dot{X}\}+[K]\{X\}=\{F_G\}+\{F_R\}+\{F_E\}+\{F_W\} \quad (1)$$

where $[M]$ is a mass matrix, $[C]$ is the damping matrix, $[K]$ is a stiffness matrix of structure, X and its derivatives are unknown vectors of 6 degree of freedom (3 translations and 3 rotations) and their derivatives. The terms in right side of the equation (1) are the external force vectors acting on the system and typically varies with time, where $\{F_G\}$ is the mooring force, $\{F_R\}$ is the hydrostatic restoring force, $\{F_E\}$ is the wave exciting force, $\{F_W\}$ is the aerodynamic force.

The mooring force is defined as follow,

$$\{F_G\}=-[K_G]\{X\} \quad (2)$$

where the mooring stiffness $[K_G]$ is determined based on a result of catenary analysis from the steady forces, i.e. tidal current force, wind force and wave drift force.

Under assumption of infinitesimal displacement theory, hydrostatic restoring force can be simplified by the first-order hydrostatic restoring force coefficient $[K_R]$ [5] as follow.

$$\{F_R\}=-[K_R]\{X\} \quad (3)$$

$$[K_R]=\begin{bmatrix} 0 & 0 & 0 & 0 & 0 & 0 \\ 0 & 0 & 0 & 0 & 0 & 0 \\ 0 & 0 & -\rho_w g A_w & 0 & 0 & 0 \\ 0 & 0 & 0 & -W\times GM_X & 0 & 0 \\ 0 & 0 & 0 & 0 & -W\times GM_Y & 0 \\ 0 & 0 & 0 & 0 & 0 & 0 \end{bmatrix} \quad (4)$$

where ρ_w is the density of water, g is the gravity acceleration, A_w is the still surface area, W is the weight of model, GM_X and GM_Y are the meta-center height in the X and Y direction, respectively.

In order to calculate the wave exciting force on the floating structure, the modified Morison's equation by Sarpkaya et al. [6] can be adapted as shown in the equation (5).

$$F_E=0.5\rho_w C_D D u_r|u_r|\Delta L+\rho_w\left[(C_M-1)\dot{u}_r+\dot{u}\right]A\Delta L \quad (5)$$

$$=0.5\rho_w C_D D\Delta L\left(u-\dot{X}\right)\left|u-\dot{X}\right|+\rho_w C_M A\Delta L\dot{u}-\rho_w\left(C_M-1\right)A\Delta L\ddot{X} \quad (6)$$

$$=F_{ED}+F_{EW}+F_{EM} \quad (7)$$

$$F_{EM}=M_E\ddot{X} \quad (8)$$

where the first term F_{ED} is the drag force, the second term F_{EW} is in proportion to the wave particle acceleration and the third term is the added inertia force, M_E is called as added mass coefficients. Here, ΔL is the length of the column, u_r and $\dot{u}_r$ is the relative wave particle velocity and relative wave particle acceleration. $\dot{X}$ is the velocity of the moving element, C_D and C_M are the hydrodynamic drag and inertia coefficients, respectively, D is a typical reference dimension of the floating column, u is the wave particle velocity of water, and $\dot{u}$ is the wave particle acceleration of water. The drag and inertia coefficients depend on the cross-sectional shape of the structure, was commonly given as constant values, $C_D=1.17$ and $C_M=2.0$ for the cylindrical structure members, $C_D=2.05$ and $C_M=2.29$ for the rectangle structure members by Motora et al. [5]. Hendeson et al.[1] and Offshore Standard DNV-OS-J101[7] showed that those values were in general the functions of the Reynolds number $\mathrm{Re}=u_{\max}D/\nu$, the Keylegan-Carpenter number $K_c=u_{\max}T/D$ and the relative

roughness, where $u_{\max}$ is the maximum wave particle velocity at still water lever, ν is the kinematic viscosity of water, T is the period of the waves.

Since the relative wave particle velocity as well as the first term of the wave exciting force contains the velocity of the moving element, the hydrodynamic damping is automatically taken into account during the simulation.

The Morison's equation is well known in estimation of the exciting force in the perpendicular to the slender columns, especially for offshore structures with fixed cylinder foundation in civil engineering. However, it cannot predict accurately forces acting on the bottom of the vertical cylinder. In this study, the added inertia force acting on the bottom of the base floater is defined by the haft sphere proposed by Haslum [8] as shown in equation (9), where D is the diameter of the bottom of the base floater.

$$M_E = \rho_w (C_M - 1) 2\pi/3 (D/2)^3 \tag{9}$$

Moreover, the damping force as the effect from the bottom of the vertical cylinder is assumed by equation (10), where $\dot{X}_i (i=3)$ is the velocity of the moving element in the vertical direction and $[C_{ED}]$ is a damping matrix. This damping force can be modeled by a pseudo structural damping of the system in the vertical direction.

$$\{F_{ED}\} = -[C_{ED}]\{\dot{X}_i\} \qquad (i=3) \tag{10}$$

The quasi-steady aerodynamic theory is used in calculation of the aerodynamic forces, in which the drag, the lift force and the moment are estimated by using aerodynamic coefficients and the relative wind speed as follows.

$$\{F_W\} = \{F_D, F_L, F_M\} \tag{11}$$

$$F_D = 0.5\rho d C_D(\alpha) V^2 \tag{12}$$

$$F_L = 0.5\rho d C_L(\alpha) V^2 \tag{13}$$

$$F_M = 0.5\rho d^2 C_M(\alpha) V^2 \tag{14}$$

where ρ is the density of air, d is a reference dimension of the wind turbine, C_D is the aerodynamic drag coefficient, C_L is aerodynamic lift coefficient, C_M is aerodynamic moment coefficient, α is angle of attack of the relative wind speed V. Here, the relative wind speed with respect to the moving element can be written as

$$V = U - \dot{X} \tag{15}$$

where, U is the wind velocity, $\dot{X}$ is the velocity of the moving element. Since the relative wind speed as well as aerodynamic force terms contains the velocity of the moving element, the aerodynamic damping is automatically taken into account during the simulation.

2.2 *Numerical scheme*

In this study, in order to solve the equation (1), the mooring force, hydrostatic restoring force and the added inertia force were moved to left side of the equation. The equation (1) can be rewritten as,

$$([M]+[M_E])\{\ddot{X}\} + ([C]+[C_{ED}])\{\dot{X}\} + ([K]+[K_G]+[K_R])\{X\} = \{F_{ED}\} + (F_{EW}) + \{F_W\} \tag{16}$$

A FEM code based on equation (16) was developed to predict the eigen-periods and dynamic responses of the floating offshore wind turbine system. A brief description of the code is summarized in Table 1. The beam elements were used for the discretization and the mass of each element was concentrated at its nodes constructing a symmetrical lumped mass matrix.

The damping matrices is defined by Rayleigh damping method [9] and it can be written as follows,

$$[C] = \alpha[M] + \beta[K] \tag{17}$$

$$[C_{ED}] = \alpha_1([M]+[M_E]) + \beta_1[K] \tag{18}$$

where α, β is the function of the eigen-periods and structural damping ratios, α_1, β_1 is the function of the eigen-periods and damping ratios of the system in the vertical direction.

Table 1. A brief description of the FEM code

Dynamic analysis	Direct numerical integration, the Newmark method
Eigenvalue analysis	Subspace iteration procedure
Element type	Beam element
Formulation	Total Lagrangian formulation
Damping	Rayleigh damping

3 NUMERICAL RESULTS

In order to evaluate the performance of the developed FEM code, a floating offshore wind turbine system model with the beam elements was constructed using the structural properties of experimental model [3] including 186 nodes and 188 elements, where the floater has 48 nodes and 50 elements, and each wind turbine has 47 nodes and 46 elements (figure 1). Here, the mooring was simplified by the longitudinal linear spring.

An eigenvalue analysis was carried out and the eigen-periods were compared with the natural periods of the free vibration test to confirm the constructed model. Then the free vibration test was reproduced by dynamic simulation to predict the damping ratios of the system in the vertical direction. In order to evaluate the performance of the developed code, the dynamic simulations were also conducted in the same condition of the experiment and the predicted responses were compared with those from the water tank test.

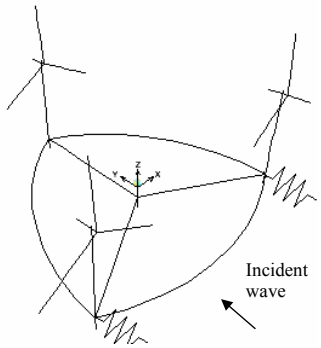

Figure 1. Model of beam elements

In the analysis, the hydrodynamic drag and inertia coefficients were defined as the functions of Kevlegan-Carpenter number recommended by Offshore Standard DNV-OS-J101[8]. Here, these coefficients of the rectangle connecting girders were revised from the ratios of those constant values that was defined by Motora et al.[5] between rectangle and cylinder columns. Where the Kevlegan-Carpenter number was simplified by the incident wave height and diameter of column by the equation (19).

$$K_c = UT/D = \pi H/D \tag{19}$$

For calculating the aerodynamic force, the aerodynamic drag coefficient of 0.6, 0.6 and 1.3 was used for the tower, nacelle and blades respectively in the survival condition, and the rotor was modeled by the axial force acting on the hub of wind turbine with thrust coefficient Ct=0.33 corresponding to the operating condition. The wave particle velocities and accelerations were generated from the linear Airy wave potential flow function.

Three dynamic simulations were carried out for the wave periods of 0.1~3.0s by a period increment of 0.1s, the wave height of H=2, 4 and 8cm and without wind to investigate the effect of wave to the dynamic behavior of floater, with wind speed U=2m/s in the operating case and with wind speed U=4m/s in the survival case to evaluate the effect of aerodynamic damping to floater. The incident wave direction was 90 degree as shown in figure 1. Each simulation was carried out for 70s by a time increment of 0.05s and the first 10s time series results were omitted for the evaluation of

the results. The responses in surge, heave and pitch directions were output and evaluated to make clear the characteristics of model and for comparison with the experiments.

3.1 *Free vibration simulation*

Table 1 presents the natural periods of the floating offshore wind turbine system obtained from the free vibration test and those form the eigenvalue analysis using the model with the beam elements. The eigen-periods of surge and heave show a good agreement with the natural periods from the free vibration test, indicated that the eigen-period of surge corresponding to the period from mooring system, and the eigen-period of heave corresponding to the vertical motion.

Table 2. Comparison of measured and predicted natural periods of the floating model of offshore wind turbine system

Direction	Natural periods from free vibration test (s)	Periods from eigenvalue analysis (s)
Heave (Z)	3.00	3.06
Surge (Y)	2.87	2.82

In order to evaluate the ability of the Morison equation to predict the dynamic responses of floater, the free vibration was demonstrated and the results were compared with the free vibration test. Figure 2 shows the comparison of the time series of surge and heave from the free vibration test and dynamic simulation. The predicted surge show a good agreement with experimental results, indicate that the damping force in the surge direction can be simulated well by Morison equation. On the other hand, the heave is overestimated by using the Morison equation and quite good agreement when the damping force in the equation (10) was added with damping ratio 6.0% of the vertical motion.

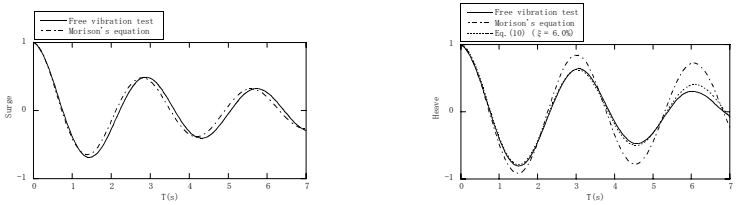

(a) Surge (b) Heave

Figure 2. Comparison of the time series of responses from free vibration test and dynamic simulation

3.2 *Prediction of dynamic responses*

Figure 3 presents variations of normalized responses with the wave periods from numerical simulation comparing with experimental results in the case without wind. As expected, the predicted responses vary linearly with the wave height in the ranges of periods far from the eigen-periods. But the predicted responses, specially, surges normalized by wave heights show significant peak around the eigen-period, decrease significantly when wave heights increase, and those show a good agreement with experimental results.

To investigate these characteristics, the forces in the equation (16) normalized by wave heights were calculated. Figure 5 and 6 present the time series of the forces in the surge direction with the incident wave height of H=2cm, 4cm, 8cm and wave period of T=2.0s, 2.8s, where the F_M, F_C, F_K are the first, second and the third term of the left side of equation (16) as the inertia force, damping force and restoring force respectively. Here, the wind load F_W is zero.

In the case of wave period 2.0s, the contributions of normalized forces in the equation (16) are almost the same in the cases of wave height H=2cm, 4cm and 8cm. In addition, the damping and hydrodynamic drag forces are small enough to be neglected in comparison with other ones. Therefore, the equation can be linearized by the wave height, and the predicted surges will be linear with the wave height in the wave period of 2.0s corresponding to the period far from the eigen-periods.

On the other hand, the normalized inertia and restoring forces decrease, the hydrodynamic drag forces increase with the incident wave heights in the case of wave period 2.8s corresponding to the eigen-period of surge. It indicated that the contributions of hydrodynamic drag forces are large, and the equation (16) cannot be linearized by the wave height in the case.

Therefore, the normalized surges do not depend on the wave height in the wave periods far from eigen-periods, because the hydrodynamic drag forces are small enough. But they decrease around the eigen-periods due to the increase of the hydrodynamic drag forces with the incident wave heights in wave periods.

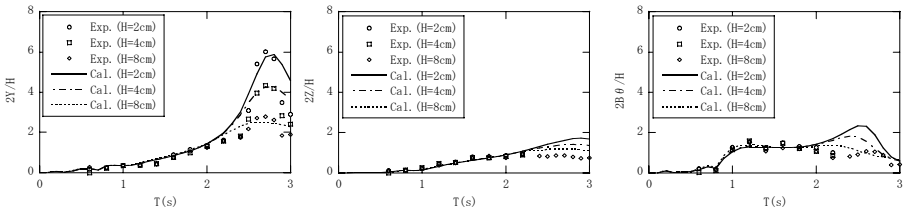

(a) Surge (b) Heave (c) Pitch

Figure 3. Variations of normalized responses with the wave periods from numerical simulation comparing with experimental results

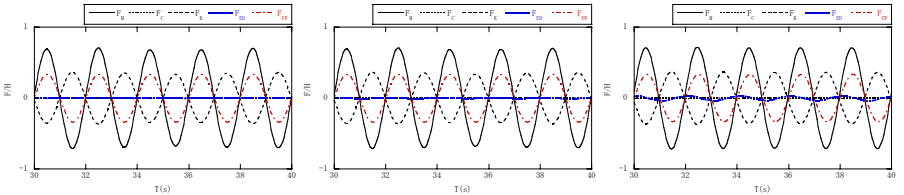

(a) H=2cm (b) H=4cm (c)H=8cm

Figure 4. Time series of forces acting on the model in surge direction (T=2.0s)

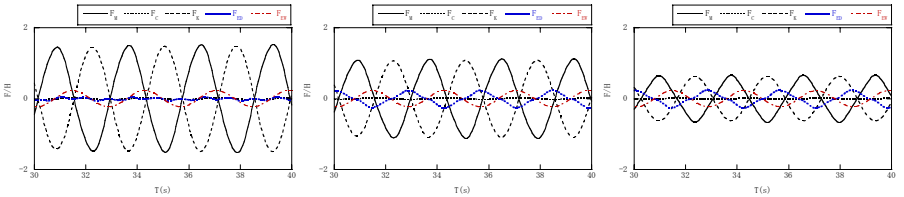

(a) H=2cm (b) H=4cm (c)H=8cm

Figure 5. Time series of forces acting on the model in surge direction (T=2.8s)

4 THE CHARACTERISTICS OF DYNAMIC RESPONSES OF SEMI-SUBMERSIBLE FLOATER

4.1 *The effect of hydrodynamic damping*

As mention above, hydrodynamic drag force is an important factor to simulate the critical peak responses of floating structures. Figure 6 shows the variations of normalized surge with the wave periods using different hydrodynamic drag coefficients as zero *(Cd=0)*, constant *(Cd=costant)* and a function of Kevlegan-Carpenter number*(Cd=f(Kc))* comparing with experimental results. When the wave period closes to the resonance period, the predicted surge is overestimated when the hydrodynamic drag coefficient is zero, and underestimated when the coefficient is constant. However, the predicted surge shows a good agreement with experiment when the hydrodynamic drag coefficient is the function of Kevlegan-Carpenter number.

4.2 *The effect of aerodynamic damping*

To investigate the effect of wind turbine to floater, a dynamic simulation was also carried out with the wind speed U=2m/s and 4m/s corresponding to the operating and survival condition, respectively. Figure 7 presents the predicted amplitude of normalized surge without wind and with wind. As the experiment [3], around the resonant point, the predicted peak responses at the wind speed U=2m/s are less than those without wind, and the effect of the aerodynamic damping is more significant for the cases with smaller wave height having lower hydrodynamic damping. It indicates that the surges around resonant point will be overestimated when the interaction between wind turbines and floater are neglected, which be done in the conventional numerical models.

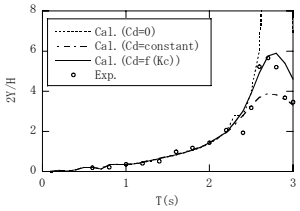

Figure 6. Effect of hydrodynamic drag coefficients to response of floater

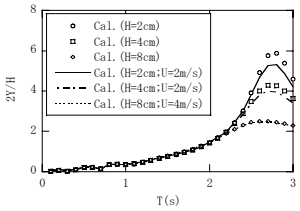

Figure 7. Effect of wind on response of floater

4.3 *The effect of elastic deformation*

To investigate the effect of elastic deformations to the dynamic response of the floater, a floating offshore wind turbine system model with the beam elements was constructed for a rigid model and an elastic model using the structural properties of the prototype floater including the number elements and nodes as the same as those of the model in the previous section. The SM570 steel material defined by Architecture Institute of Japan [10] was used for the connecting girder and other of sections were rigid in elastic model.

Table 3 shows the eigen-periods of the models. The eigen-period 26s corresponding to the mooring system, and the eigen-period 28s and 25s corresponding to the vertical motion were estimated in both rigid and elastic model. However, there are other eigen-periods that were only obtained from the deformation of elastic model.

Table 3. Comparison of eigen-periods between the elastic and rigid model.

No	1	2	3	4	5	6	7	8	9	10	11	12
Eigen-periods of Rigid Model T(s)	28	26	25	-	-	-	-	-	-	-	-	-
Eigen-periods of Elastic Model T(s)	28	26	25	11.8	9.8	6.3	6.0	4.3	3.6	3.5	3.2	2.8
Mode characteristics	Mode shapes from the mooring and restoring forces			Mode shapes from the deformation of elastic model								

The dynamic simulations of both models were also performed in the regular wave periods from 1.0s~30.0s with the wave height of 12m in the survival condition. The structural damping ratio of floater was 0.8% for the steel material as mentioned by Burton et al.[11], and damping ratio of the vertical motion was 6%. The incident wave direction was -90 degree. Figure 8 and 9 presents the variations of normalized responses with the wave periods of the elastic model comparing with rigid model at the central floater and upstream base floater, respectively.

The surge of the elastic model is the same with those of rigid model. On the other hand, the peak of heave can be found at the periods near 10s and 6s, corresponding to the eigen-periods of the mode at the deformation of elastic model. However, the normalized heave of rigid and elastic model are in agreement when the wave period is far from these periods. It indicated that, the responses and stresses would be underestimated when the model was assumed to be a rigid body without any elastic deformation.

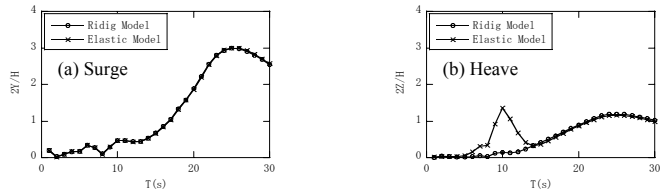

Figure 8. Variations of normalized responses with the wave periods of the elastic model comparing with rigid model at the central floater

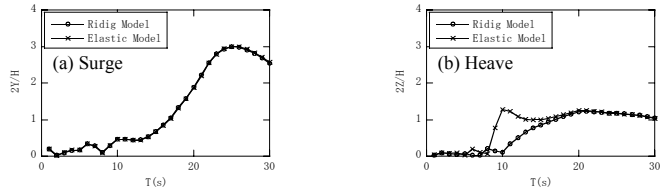

Figure 9. Variations of normalized responses with the wave periods of the elastic model comparing with rigid model at the downstream base floater

5 SUMMARY AND CONCLUSIONS

A FEM code was developed for the analysis of dynamic responses of the floating offshore wind turbine system in consideration of the interaction between the wind turbines and the floater. The predicted responses showed good agreement with the experiments, indicating the hydrodynamic damping play an important role at the resonant points and the hydrodynamic coefficients should be the function of Kevlegan-Carpenter number. In addition, the responses will be overestimated without considering the interaction between wind turbines and floater .The dynamic responses of rigid and elastic floater were also investigated, and the results indicated that the responses of elastic model showed some peaks around the eigen-periods of elastic deformation that would not be observed in the assumption of rigid without any elastic deformation.

REFERENCES

1 A. Henderson, M. Patel, Rigid-Body Motion of a floating offshore wind farm, Int. Journal of Ambient Energy, Vol.19, No.3, pp 167-180, 1998.
2 B.H. Bulder, M.Th. van Hees, A. Hendeson, R.H.M. Huijsmans, J.T.G. Pierik, E.J.B. Snijders, G.H.Wijnants, and M.J.Woft, Study to feasibility of and boundary conditions for floating offshore wind turbines, Public report 2002-CMC-R43, ECN, MARIN, MSC, Lagerwey the Windmaster, TNO, TUD, 2002.
3 T. Ishihara, P.V. Phuc, H. Sukegawa, K. Shimada, T. Ohyama, A study on the dynamic response of a semi-submersible floating offshore wind turbine system Part 1: water tank test with considering the effect of wind load, ICWE12, Australia 2007.
4 Architectural Institute of Japan, Recommend for Structural Design of the Oceanic Architecture (Floating-Type Structure), 1990.
5 S.Z. Motora, T.O. Koyama, M.T. Fujino, H.A. Maeda, Dynamics of ships and offshore structures, 1997.
6 T. Sarpkaya, M. and Isaacson, Mechanics of wave forces on offshore structures, Van Norstrand Reinhold, 1981.
7 Offshore Standard DNV-OS-J101, Design of offshore wind turbine structures, 2004.
8 H.A. Haslum, Alternative Shape of Spar Platforms for Use in Hostile Areas, Offshore Technology Conference, 1999.
9 J.W. Tedesco, W.G. McDougal, C.A. Ross, Structural dynamic theory and application, Addison Wesley Longman, Inc., pp 370-371, 1998.
10 Architectural Institute of Japan, Design Standard for Steel Structures -Based on Allowable Stress Concept, 2005.
11 T. Burton, D. Sharpe, N. Jenkins, E. Bossanyi, Wind Energy Handbook, Wiley, England, 2001.